Received: 23 November 2017 | Revised: 17 March 2018 | Accepted: 11 April 2018

DOI: 10.1002/dac.3703

RESEARCH ARTICLE

WILEY

Channel modeling and analysis for multipolarized massive MIMO systems

Xudong Cheng | Yejun He | Li Zhang | Jian Qiao

Shenzhen Key Laboratory of Antennas and Propagation, College of Information Engineering, Shenzhen University, Shenzhen 518060, China

Correspondence
Yejun He, Shenzhen Key Laboratory of Antennas and Propagation, College of Information Engineering, Shenzhen University, Shenzhen 518060, China.
Email: heyejun@126.com

Funding information
National Natural Science Foundation of China, Grant/Award Number: 61372077; Shenzhen Science and Technology Programs, Grant/Award Numbers: ZDSYS 201507031550105, JCYJ 20170302150411789, JCYJ 20170302142515949 and GCZX 2017040715180580; Guangdong Provincial Science and Technology Program, Grant/Award Number: 2016B090918080; China Postdoctoral Science Foundation, Grant/Award Number: 2016M602519; Guangzhou Science and Technology Program, Grant/Award Number: 201707010490

Summary

In this paper, we use the multipolarized antennas in massive multiple-input multiple-output (MIMO) systems to decline the channel orthogonality and enhance the system performance. We propose 3 multipolarized massive MIMO system schemes according to antenna structures of 3 widely used massive MIMO systems and establish 3-D geometrical channel models. Simulation results show that the multipolarized massive MIMO systems outperform the unipolarized massive MIMO systems in many situations. The multipolarized antennas would be the best choice for massive MIMO systems if the space efficiency and the miniaturization of equipments are of primary concern.

KEYWORDS

channel model, favorable propagation, massive MIMO, multipolarized antenna

1 | INTRODUCTION

As we all know, the massive multiple-input multiple-output (MIMO) systems have been regarded as a candidate technology for the 5th generation cellular networks, which have attracted considerable research interests recently. Massive MIMO systems have a base station (BS) equipped with a large number of antennas (tens or hundreds of antennas), which can serve several single antenna users simultaneously.[1-3] The favorable propagation characteristic, which is also called channel orthogonality between different users, should be considered in massive MIMO systems,[4] which plays a key role in massive MIMO systems performance[5] and it is very different from the classic MIMO Rayleigh fading channel.[6] A high channel orthogonality means that the users cannot use the same frequency resource at the same time,[7] while a low channel orthogonality (favorable propagation) can reduce the cross-talk between users and simplify the precoding of massive MIMO systems, which is beneficial to the channel capacity. Since the massive MIMO systems have a large-scale antenna array, a large number of antennas are difficult to be placed in a limited space, and if it can be deployed, the high channel orthogonality may degrade the systems performance because of the space and size restrictions.[8] In the traditional MIMO systems, the multipolarized antennas have been implemented to reduce the correlation between antennas and realize the space efficiency because an antenna is designed to receive a signal having

a certain polarization and it is completely isolated to the cross-polarization component. Also, the implementation of multipolarized antennas in MIMO systems is helpful with significant performance improvements.[9] Therefore, we use the multipolarized antennas in massive MIMO systems to decline the channel orthogonality and improve the systems performance and the space efficiency.

So far, a lot of works have been done in developing massive MIMO systems. Previous studies[10-14] investigated how massive MIMO systems perform in channels measured in real propagation environments and obtained lots of real measurements, while many other works[15-17] focused on the massive MIMO systems channel modeling because performing experiments is expensive and time-consuming and some particular parameters are difficult to measure. However, these models are complex, and most of the research works[4,18,19] are based on idealized channel matrix assumption using independent and identically distributed Rayleigh fading channels, which are impractical in reality. Also, there are very few works about multipolarized antennas used in massive MIMO systems. Xu et al[20] considered a multicell network with BS equipped with large dual-polarized antenna arrays, and it found that a dual-polarized system enjoys the reduction in pilot contamination and multiuser interference due to orthogonal polarizations. Park and Clerckx[8] have investigated a dual-structured linear precoding in the multipolarized multiuser massive MIMO system to reduce the feedback overhead further. Xiao et al[21] studied how to optimize dual-stage precoding scheme in a typical dual-polarized massive MIMO system and proposed a specific structure of long-term precoding matrix for dual-polarized massive MIMO systems.

In this paper, we propose 3 multipolarized massive MIMO system schemes according to antenna structures of 3 widely used massive MIMO systems such as uniform linear array (ULA), uniform circular array (UCA), and uniform rectangular array (URA). Then we establish 3-D geometrical channel models for multipolarized ULA, UCA, and URA massive MIMO systems. The channel is modeled as a Ricean fading channel that includes a fixed (line of sight, LoS) part and a scattering (non-LoS) part. Both the azimuth angle of arrival (AAoA) and the elevation angle of arrival (EAoA) have been taken into account. We use the uniform distribution with certain azimuth angle spread (AAS) and elevation angle spread (EAS) to characterize the AAoA/EAoA distributions. For the system performance, we focus on the channel orthogonality and channel capacity. Simulation results show that using multipolarized antennas in massive MIMO systems can help to decline the channel orthogonality between users and reduce the demand for large antenna spacing to realize the space efficiency compared with the unipolarized massive MIMO systems. The multipolarized massive MIMO systems have better performance than the unipolarized massive MIMO systems in many situations. While when the signal-to-noise ratio (SNR) is low, multipolarized massive MIMO systems do not outperform unipolarized massive MIMO systems because of the power loss and imbalance between antennas due to the polarization mismatch. For the 3 kinds of multipolarized massive MIMO systems, the multipolarized ULA massive MIMO systems have the best performance because of the long line antenna structure while the multipolarized URA massive MIMO systems have the worst performance because of the compact antenna structure.

The remainder of this paper is organized as follows. Section 2 is about the channel modeling of multipolarized ULA massive MIMO systems. In Section 3, the multipolarized UCA massive MIMO systems are modeled. Section 4 models the multipolarized URA massive MIMO systems. Section 5 gives the simulation result comparisons and analysis. Finally, we present the concluding remarks in Section 6.

2 | 3-D CHANNEL MODELING OF MULTIPOLARIZED ULA MASSIVE MIMO SYSTEMS

A typical massive MIMO system has a BS equipped with M antennas as shown in Figure 1, where M antennas serve K ($K<M$) single antenna users simultaneously. The M BS antenna structures can be ULA, UCA, and URA, and the K single antenna users are at random positions in the same cell. Usually, wireless channel can be modeled as a Ricean fading channel, which means the channel matrix is composed of a fixed (LoS) part and a scattering (non-LoS) part according to[22]

$$\mathbf{H} = \sqrt{\frac{k}{k+1}}\bar{\mathbf{H}} + \sqrt{\frac{1}{k+1}}\tilde{\mathbf{H}} \in \mathbb{C}^{M\times K}, \tag{1}$$

where k is the Ricean k-factor and it is defined as the power ratio of the fixed part to the scattering part. $\bar{\mathbf{H}}$ is a deterministic matrix representing the fixed part, and $\tilde{\mathbf{H}}$ is a random matrix representing the scattering part. As mentioned above, for massive MIMO systems, the favorable propagation (ie, channel orthogonality between different users) is the most important property; namely,[23]

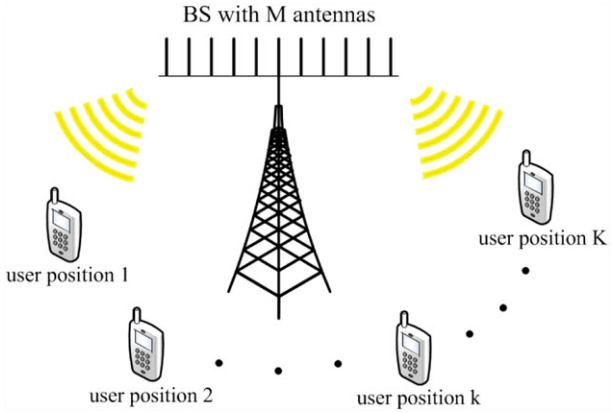

FIGURE 1 Massive multiple-input multiple-output system with a base station (BS) of M antennas and K user positions

$$\frac{1}{M}\mathbf{h}_p^H\mathbf{h}_q \underset{M\to\infty}{\overset{a.s.}{\to}} \begin{cases} 0, & p\neq q \\ 1, & p=q, \end{cases} \tag{2}$$

where $\mathbf{h}_k(k=1,...,K)$ is the channel vector using M antennas of the BS at user terminal position k, H denotes the Hermitian transform, and $\overset{a.s.}{\longrightarrow}$ is almost sure convergence. For $\frac{1}{M}\mathbf{h}_p^H\mathbf{h}_q \underset{M\to\infty}{\overset{a.s.}{\to}} 0(p\neq q)$, it means that the channel offers favorable propagation, while $\frac{1}{M}\mathbf{h}_p^H\mathbf{h}_q \underset{M\to\infty}{\overset{a.s.}{\to}} 1(p\neq q)$ means the 2 users cannot use the same frequency resource at the same time. Therefore, we first consider the scattering part (or channel)—a 3-D multipolarized ULA massive MIMO system transmission scenario as shown in Figure 2. Usually, we regard the ground as a reference, which means the antennas perpendicular to the ground are vertically polarized antennas and the antennas parallel to the ground are horizontally polarized antennas.[24] The $x-S_1-y$ plane is the horizontal plane. Hence, antennas A_1 and A_m are vertically polarized antennas, antennas A_2 and A_{m+1} are horizontally polarized antennas, and we make vertically polarized antennas and horizontally polarized antennas are arranged alternately. This means in our proposed multipolarized ULA massive MIMO systems scheme, if all the odd numbered antennas are vertically polarized antennas, all the even numbered antennas will be horizontally polarized antennas and vice versa. All the antennas are in the far field of the signals; therefore, the wave front is plane wave, and the signals come from arbitrary directions with AAoA α and EAoA β for all the antennas. The adjacent antenna spacing is d. For antenna A_2, $S_2P_2^{'}$ is the projection of S_2P_2 on the horizontal plane. $\angle P_2S_2P_2^{'}$ is β, and $\angle P_2^{'}S_2S_1$ is $(\pi/2-\alpha)$. Therefore, the angle $\angle P_2S_2S_1$ can be defined as[25]

$$\begin{aligned} \cos\angle P_2S_2S_1 &= \cos\angle P_2^{'}S_2S_1\cos\angle P_2S_2P_2^{'} \\ &= \cos(\pi/2-\alpha)\cos(\beta). \end{aligned} \tag{3}$$

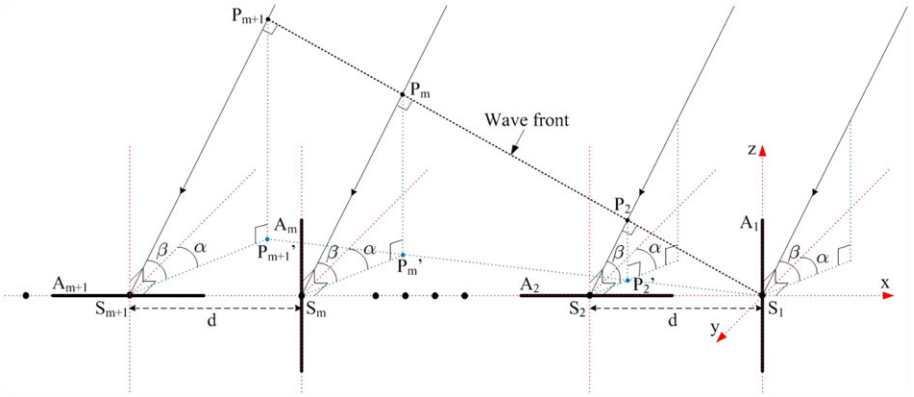

FIGURE 2 3-D multipolarized uniform linear array massive multiple-input multiple-output system transmission scenario

The transmission distance difference between antennas A_1 and A_2 is P_2S_2. Regarding antenna A_1 as a reference antenna, one path of multipath channels at antennas A_1 and A_2 can be expressed as

$$h_1^{\mathrm{ULA}} = \sqrt{P_{\mathrm{V}}}e^{j\phi}, \tag{4}$$

$$h_2^{\mathrm{ULA}} = \sqrt{P_{\mathrm{H}}}e^{j(\phi+2\pi d\cos(\frac{\pi}{2}-\alpha)\cos(\beta)/\lambda)}, \tag{5}$$

where P_{V} and P_{H} are vertically polarized power and horizontally polarized power in this path, respectively, and ϕ is random phase and it is independent and identically distributed uniform random variable on the interval $[-\pi,\pi)$.[26] λ is the carrier wavelength.

$$\mathbf{h}_p^{\mathrm{ULA}} = \begin{bmatrix} h_{1,p}^{\mathrm{ULA,XPD}} \\ h_{2,p}^{\mathrm{ULA,XPD}} \\ \cdots \\ h_{m,p}^{\mathrm{ULA,XPD}} \\ h_{m+1,p}^{\mathrm{ULA,XPD}} \\ \cdots \end{bmatrix} = \begin{bmatrix} \sqrt{P_{\mathrm{V}}(1-a)}e^{j\phi_p} \\ \sqrt{P_{\mathrm{V}}a}e^{j(\phi_p+2\pi d\cos(\frac{\pi}{2}-\alpha_p)\cos(\beta_p)/\lambda)} \\ \cdots \\ \sqrt{P_{\mathrm{V}}(1-a)}e^{j(\phi_p+2\pi d(m-1)\cos(\frac{\pi}{2}-\alpha_p)\cos(\beta_p)/\lambda)} \\ \sqrt{P_{\mathrm{V}}a}e^{j(\phi_p+2\pi dm\cos(\frac{\pi}{2}-\alpha_p)\cos(\beta_p)/\lambda)} \\ \cdots \end{bmatrix}, \tag{6}$$

$$\mathbf{h}_q^{ULA} = \begin{bmatrix} h_{1,q}^{\mathrm{ULA,XPD}} \\ h_{2,q}^{\mathrm{ULA,XPD}} \\ \cdots \\ h_{m,q}^{\mathrm{ULA,XPD}} \\ h_{m+1,q}^{\mathrm{ULA,XPD}} \\ \cdots \end{bmatrix} = \begin{bmatrix} \sqrt{P_{\mathrm{H}}a}e^{j\phi_q} \\ \sqrt{P_{\mathrm{H}}(1-a)}e^{j(\phi_q+2\pi d\cos(\frac{\pi}{2}-\alpha_q)\cos(\beta_q)/\lambda)} \\ \cdots \\ \sqrt{P_{\mathrm{H}}a}e^{j(\phi_q+2\pi d(m-1)\cos(\frac{\pi}{2}-\alpha_q)\cos(\beta_q)/\lambda)} \\ \sqrt{P_{\mathrm{H}}(1-a)}e^{j(\phi_q+2\pi dm\cos(\frac{\pi}{2}-\alpha_q)\cos(\beta_q)/\lambda)} \\ \cdots \end{bmatrix}. \tag{7}$$

In real wireless channel, the reflections, diffractions, and scatterings of signals in the wireless channel may result in channel depolarization, which means the polarization orientation may change and rotate after passing through the channel (ie, a vertically polarized signal at transmitter may have horizontally polarized component at receiver). A commonly used method for describing this phenomenon is to define the cross-polarization discrimination (XPD)[27]:

$$\mathrm{XPD} = \frac{\mathrm{E}\{|h_{VV}|^2\}}{\mathrm{E}\{|h_{HV}|^2\}} = \frac{\mathrm{E}\{|h_{HH}|^2\}}{\mathrm{E}\{|h_{VH}|^2\}} = \frac{1-a}{a}, \tag{8}$$

where $h_{XY}(X,Y\in V,H)$ is XY channel and E{} represents the expectation operator. $a(0<a\leq 1)$ is defined for modeling and computing, which corresponds to the part of the power that is leaked from X polarization to Y polarization.[24] When there is no leakage from the X polarization to the Y polarization, a equals to 0; otherwise, there is leakage between the polarizations when $0<a\leq 1$. Then the one path channel including XPD can be expressed as

$$h_1^{\mathrm{ULA,XPD}} = \sqrt{P_{\mathrm{V}}(1-a)+P_{\mathrm{H}}a}e^{j\phi}, \tag{9}$$

$$h_2^{\mathrm{ULA,XPD}} = \sqrt{P_{\mathrm{H}}(1-a)+P_{\mathrm{V}}a}e^{j(\phi+2\pi d\cos(\frac{\pi}{2}-\alpha)\cos(\beta)/\lambda)}, \tag{10}$$

where $P_X(1-a)$ is the power maintain in the copolarization and P_Xa is the power leakage to the cross-polarization.[28] In ULA massive MIMO systems, all the antennas are uniformly spaced[29,30]; therefore, for antenna A_m, one path of multipath channels can be expressed as

$$\begin{aligned} h_m^{\mathrm{ULA,XPD}} =& \sqrt{P_{\mathrm{V}}(1-a)+P_{\mathrm{H}}a} \\ & \times e^{j(\phi+2\pi d(m-1)\cos(\frac{\pi}{2}-\alpha)\cos(\beta)/\lambda)}. \end{aligned} \tag{11}$$

For the K single antenna users, it is reasonable to assume that half of the users are vertically polarized antenna users and half of the users are horizontally polarized antenna users at one moment because of the random positions.[8] Therefore, for user p with single vertically polarized antenna, the channel vector of multipolarized ULA massive MIMO systems can be written as (6). In the same way, the channel vector of user q with single horizontally polarized antenna is (7). Therefore, the complete scattering channel matrix of multipolarized ULA massive MIMO systems is

$$\tilde{\mathbf{H}}^{\mathrm{ULA}} = \left[\mathbf{h}_1^{\mathrm{ULA}}, \mathbf{h}_2^{\mathrm{ULA}}, \ ..., \mathbf{h}_p^{\mathrm{ULA}}, \ ..., \mathbf{h}_q^{\mathrm{ULA}}, \ ..., \mathbf{h}_K^{\mathrm{ULA}}\right]. \tag{12}$$

For multipath channel, many distributions can be used to characterize the AAoA/EAoA distributions. Here we use the uniform distribution with certain AAS and EAS to characterize the AAoA/EAoA distributions because many communication scenarios are consistent with uniform distribution especially in the 5th generation small cell scenario,[31] which is defined as

$$p(\Theta) = \frac{1}{2\Delta\Theta}, -\Delta\Theta + \Theta_0 \le \Theta \le \Delta\Theta + \Theta_0, \tag{13}$$

where Θ_0 is the mean AAoA/EAoA and $\Delta\Theta$ is the AAS/EAS. After getting the scattering channels and the AAoA/EAoA distributions, we can derive the orthogonality between 2 channel vectors $\mathbf{h}_p^{\mathrm{ULA}}$ and $\mathbf{h}_q^{\mathrm{ULA}}$, which is computed as[18]

$$\delta_{p,q}^{\mathrm{ULA}} = \frac{|(\mathbf{h}_p^{\mathrm{ULA}})^H \mathbf{h}_q^{\mathrm{ULA}}|}{\|\mathbf{h}_p^{\mathrm{ULA}}\| \cdot \|\mathbf{h}_q^{\mathrm{ULA}}\|}, \tag{14}$$

where $\|\cdot\|$ denotes the Euclidean norm. The low channel orthogonality (favorable propagation) between different users can reduce the interference between users and simplify the precoding and signal detection algorithm of massive MIMO systems, which is beneficial to the systems performance.

Figure 3A shows the channel orthogonality of both unipolarized and multipolarized ULA massive MIMO systems varies as the number of antennas increases with different AAS. The antenna spacing is set to be $\lambda/2$, and XPD is equal to 8 dB according to the real measurements in Soma et al.[32] Both the mean AAoA and the mean EAoA are set to be 0°, and the power is normalized. We use the Monte Carlo simulation method, where we generate 10 000 samples of the channel and compute the average channel orthogonality. From Figure 3A, we can see that the channel orthogonality decreases as the number of antennas increases. The channel orthogonality is sensitive to the AAS, and a larger AAS (ie, rich scattering) results in a lower channel orthogonality. The multipolarized ULA massive MIMO systems can obtain a very low channel orthogonality compared with the unipolarized ULA massive MIMO systems even with a small AAS (ie, poor scattering). Therefore, using multipolarized antennas in massive MIMO systems can help to decline the channel orthogonality between users, especially under a poor scattering communication environment. In addition to the scattering environment, the channel orthogonality is also sensitive to the antenna spacing. Figure 3B draws the channel orthogonality varies as antenna spacing changes, and the number of antennas is set to be 100, from which we can see that the larger antenna spacing results in a lower channel orthogonality. Also the multipolarized ULA massive MIMO systems can obtain a very low channel orthogonality compared with the unipolarized ULA massive MIMO systems even when the antenna spacing is very small. Therefore, using multipolarized antennas in massive MIMO systems can reduce the demand for large antenna spacing to realize the space efficiency. Figure 4 shows that the channel orthogonality of multipolarized ULA massive MIMO systems is also sensitive to the XPD. A higher XPD can result in a lower channel orthogonality. This is because as the XPD increases, more power will maintain in the copolarization, which declines the channel orthogonality between users with different polarized antennas.

As for fixed matrix (or channel), we assume that $\bar{h}_{XX}$ is 1 and $\bar{h}_{XY}$ is 0 because there is no polarization changes and rotations in LoS part. Then we can get the channel capacity according to[30]

$$C = \max_{\mathbf{P}} \log_2 \left[\det\left(\mathbf{I} + \frac{\rho K}{M}\mathbf{H}\mathbf{P}\mathbf{H}^H\right)\right] \mathrm{bps/Hz}, \tag{15}$$

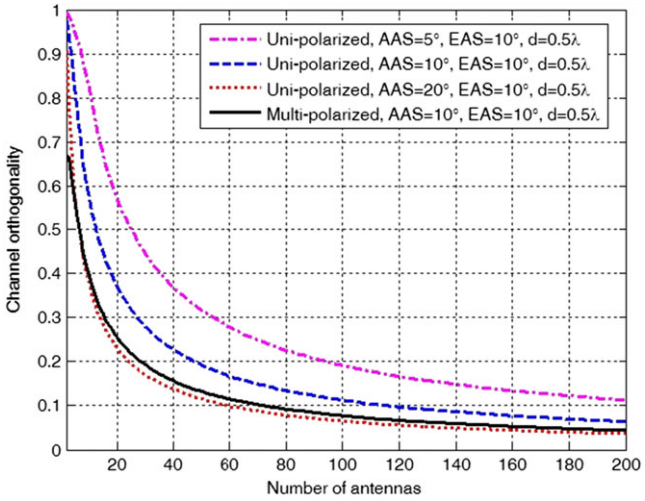

(A)

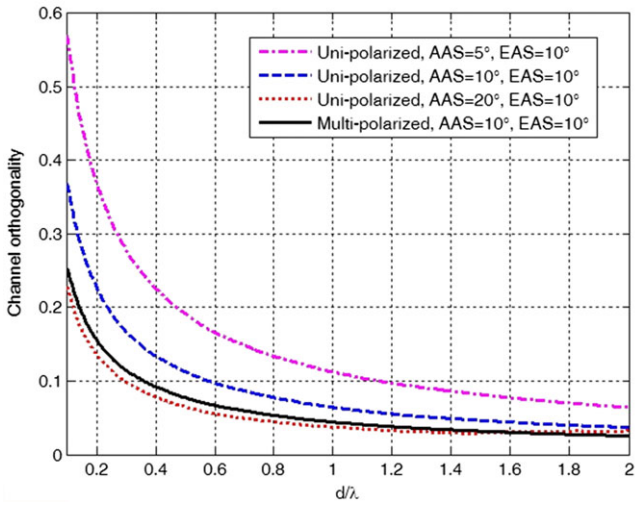

(B)

FIGURE 3 A, Channel orthogonality versus number of antennas with different AAS. B, Channel orthogonality versus antenna spacing with different AAS. AAS, azimuth angle spread; EAS, elevation angle spread

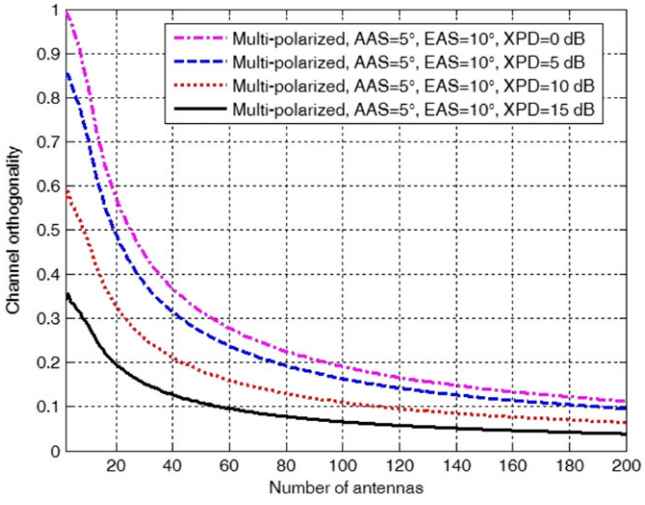

FIGURE 4 Channel orthogonality of multipolarized uniform linear array massive multiple-input multiple-output systems versus number of antennas with different XPD. AAS, azimuth angle spread; EAS, elevation angle; XPD, cross-polarization discrimination

where **I** is an identity matrix and ρ denotes the receiving SNR. **P** is a diagonal matrix for power allocation with $(p_1,...,p_k,...,p_K)$ on its diagonal and $\sum_{k=1}^{K} p_k = 1$. Figure 5 compares the channel capacity of multipolarized ULA massive MIMO systems with unipolarized ULA massive MIMO systems as AAS and antenna spacing change respectively. The antenna spacing is set to be $\lambda/2$, and the number of users is set to be 8. Cross-polarization discrimination is equal to 8 dB, and k-factor is equal to 12 dB according to the real measurements in Soma et al.[32] Signal-to-noise ratio is set to be a mean value 15 dB. From which we can see that the multipolarized ULA massive MIMO systems have larger capacity even with smaller AAS and antenna spacing, hence the multipolarized antennas implemented in massive MIMO systems can help to increase the channel capacity and improve the systems performance. Figure 6 is the comparison of capacity between multipolarized ULA massive MIMO systems and unipolarized ULA massive MIMO systems. The number of antennas is set to be 100. Figure 6 shows that the multipolarized ULA massive MIMO systems do not always outperform unipolarized ULA massive MIMO systems. In the high SNR region, the multipolarized ULA massive MIMO systems are more effective because of the reduction in the channel orthogonality between users. While in the low SNR region, the reduction in the channel orthogonality is not enough to compensate

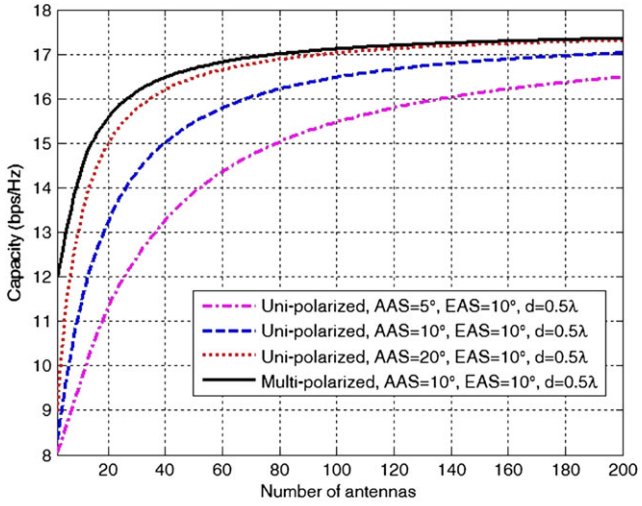

(A)

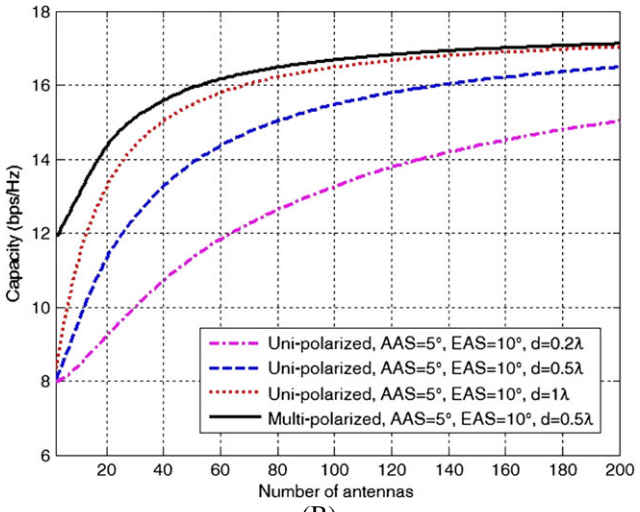

(B)

FIGURE 5 A, Channel capacity comparison of unipolarized and multipolarized uniform linear array massive multiple-input multiple-output systems versus number of antennas with different AAS. B, Channel capacity comparison of unipolarized and multipolarized uniform linear array massive multiple-input multiple-output systems versus number of antennas with different antenna spacing. AAS, azimuth angle spread; EAS, elevation angle

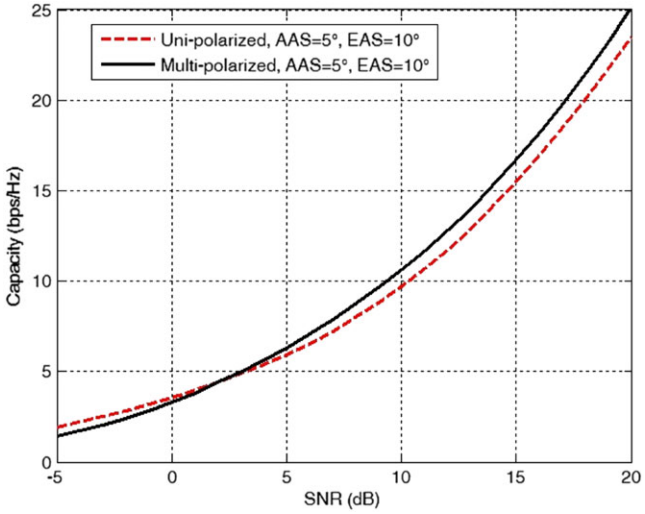

FIGURE 6 Channel capacity comparison of unipolarized and multipolarized uniform linear array massive multiple-input multiple-output systems versus SNR. AAS, azimuth angle spread; EAS, elevation angle; SNR, signal-to-noise ratio

for the power loss resulting from the polarization mismatch.[33] Hence, the multipolarized ULA massive MIMO systems have lower capacity when SNR is low.

Figure 7A shows the channel capacity of both unipolarized and multipolarized ULA massive MIMO systems varies as the XPD changes. Here we only consider the scattering channels to show the effect of XPD on the systems performance. From Figure 7A, we can see that the capacity of unipolarized ULA massive MIMO systems decreases drastically as the XPD decreases. This is because the unipolarized ULA massive MIMO systems will lose most of the power because of the polarization mismatch at low XPD. While multipolarized ULA massive MIMO systems always have cross-polarized antennas to receive the cross-polarized signals, therefore, the XPD has a slight effect on the multipolarized ULA massive MIMO systems and they achieve better performance in such situation. Figure 7B compares the channel capacity of multipolarized ULA massive MIMO systems with unipolarized ULA massive MIMO systems as *k*-factor changes. We can see that the channel capacity of both multipolarized ULA massive MIMO systems and unipolarized ULA massive MIMO systems decreases as *k*-factor increases. This is because the LoS part becomes dominant and the scattering part becomes weak as *k*-factor increases, which results in high channel orthogonality, while the multipolarized ULA massive MIMO systems outperform the unipolarized ULA massive MIMO systems as *k*-factor increases because the multipolarized ULA massive MIMO systems have low channel orthogonality even with poor scattering.

3 | 3-D CHANNEL MODELING OF MULTIPOLARIZED UCA MASSIVE MIMO SYSTEMS

The UCA is another popular antenna structure in massive MIMO systems. For multipolarized UCA massive MIMO systems, all the antennas are uniformly spaced on a circular edge as shown[11] in Figure 8. In our proposed multipolarized UCA massive MIMO systems scheme, if antenna A_m is vertically polarized antenna, antenna A_{m+1} will be horizontally polarized antenna and vice versa. Also all the antennas are in the far field of the signals, and the adjacent antenna spacing is d. According to the geometrical relationship in Figure 8, we have $\theta = \frac{2\pi}{M}, \theta_2 = \theta, \theta_3 = 2\theta, \ ..., \theta_m = (m-1)\theta, \ ...,$ and it is obvious that the circle radius r is

$$r = \frac{d}{2\sin(\theta/2)}. \tag{16}$$

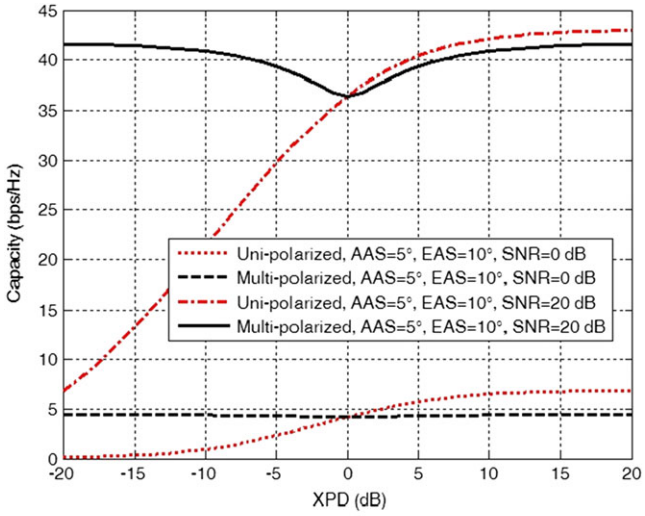

(A)

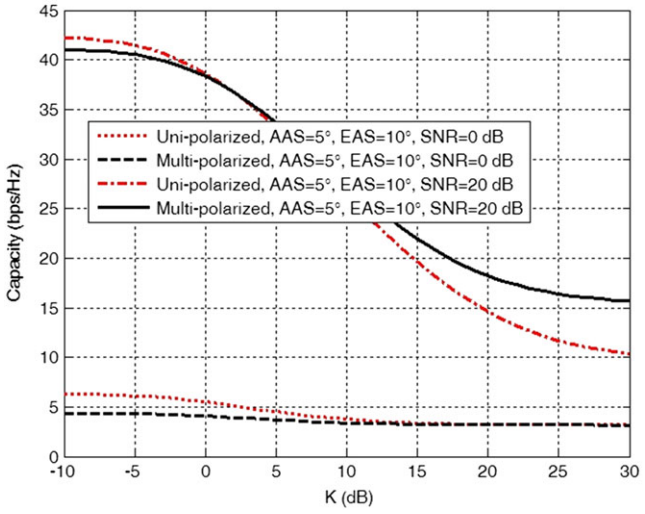

(B)

FIGURE 7 A, Channel capacity comparison of unipolarized and multipolarized uniform linear array massive multiple-input multiple-output systems versus XPD. B, Channel capacity comparison of unipolarized and multipolarized uniform linear array massive multiple-input multiple-output systems versus *k*-factor. AAS, azimuth angle spread; EAS, elevation angle; SNR, signal-to-noise ratio; XPD, cross-polarization discrimination

The distances between antenna A_1 and other antennas are

$$\begin{aligned} d_{1,2} &= \frac{d\sin(\theta_2/2)}{\sin(\theta/2)} \\ &\cdots \\ d_{1,m} &= \frac{d\sin(\theta_m/2)}{\sin(\theta/2)} \\ &\cdots \end{aligned} \tag{17}$$

$$\mathbf{h}_p^{\mathrm{UCA}} = \begin{bmatrix} h_{1,p}^{\mathrm{UCA,XPD}} \\ h_{2,p}^{\mathrm{UCA,XPD}} \\ \cdots \\ h_{m,p}^{\mathrm{UCA,XPD}} \\ h_{m+1,p}^{\mathrm{UCA,XPD}} \\ \cdots \end{bmatrix} = \begin{bmatrix} \sqrt{P_{\mathrm{V}}(1-a)}e^{j\phi_p} \\ \sqrt{P_{\mathrm{V}}a}e^{j(\phi_p+2\pi d_{1,2}\cos(\pi-\alpha_p-\arctan(\frac{r\sin\theta_2}{r-r\cos\theta_2}))\cos(\beta_p)/\lambda)} \\ \cdots \\ \sqrt{P_{\mathrm{V}}a}e^{j(\phi_p+2\pi d_{1,m}\cos(\pi-\alpha_p-\arctan(\frac{r\sin\theta_m}{r-r\cos\theta_m}))\cos(\beta_p)/\lambda)} \\ \sqrt{P_{\mathrm{V}}(1-a)}e^{j(\phi_p+2\pi d_{1,m+1}\cos(\pi-\alpha_p-\arctan(\frac{r\sin\theta_{m+1}}{r-r\cos\theta_{m+1}}))\cos(\beta_p)/\lambda)} \\ \cdots \end{bmatrix} \tag{18}$$

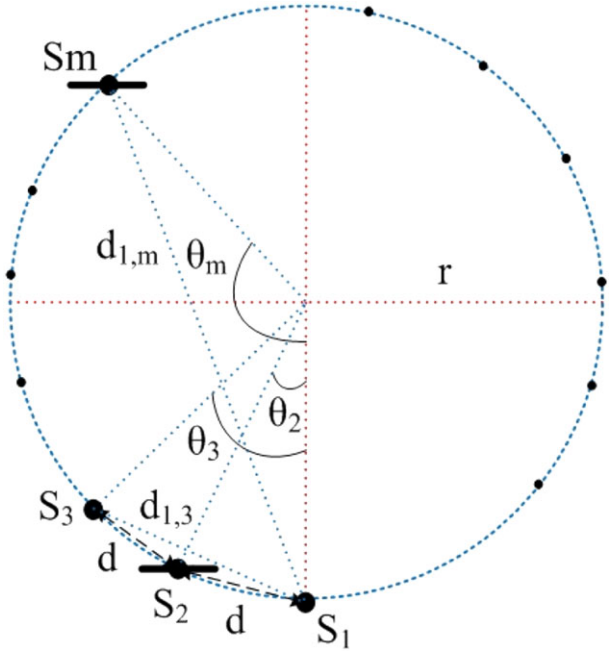

FIGURE 8 Multipolarized uniform circular array massive multiple-input multiple-output system antenna structure

$$\mathbf{h}_q^{\mathrm{UCA}} = \begin{bmatrix} h_{1,q}^{\mathrm{UCA,XPD}} \\ h_{2,q}^{\mathrm{UCA,XPD}} \\ \cdots \\ h_{m,q}^{\mathrm{UCA,XPD}} \\ h_{m+1,q}^{\mathrm{UCA,XPD}} \\ \cdots \end{bmatrix} = \begin{bmatrix} \sqrt{P_{\mathrm{H}}}ae^{j\phi_q} \\ \sqrt{P_{\mathrm{H}}(1-a)}e^{j(\phi_q+2\pi d_{1,2}\cos(\pi-\alpha_q-\arctan(\frac{r\sin\theta_2}{r-r\cos\theta_2}))\cos(\beta_q)/\lambda)} \\ \cdots \\ \sqrt{P_{\mathrm{H}}(1-a)}e^{j(\phi_q+2\pi d_{1,m}\cos(\pi-\alpha_q-\arctan(\frac{r\sin\theta_m}{r-r\cos\theta_m}))\cos(\beta_q)/\lambda)} \\ \sqrt{P_{\mathrm{H}}}ae^{j(\phi_q+2\pi d_{1,m+1}\cos(\pi-\alpha_q-\arctan(\frac{r\sin\theta_{m+1}}{r-r\cos\theta_{m+1}}))\cos(\beta_q)/\lambda)} \\ \cdots \end{bmatrix}. \tag{19}$$

For the convenience of analysis, we first analyze the relationship between antennas A_1 and A_m on the circular edge as shown in Figure 9. We can see that the transmission distance difference between the 2 antennas S_mP_m equals to $(d_{1,m}\cos\angle P_mS_mS_1)$. According to the geometrical relationship, we have

$$\begin{aligned} \cos\angle P_mS_mS_1 &= \cos\angle P'_mS_mS_1\cos\angle P_mS_mP'_m \\ &= \cos(\pi-\alpha-\angle S'_mS_mS_1)\cos(\beta), \end{aligned} \tag{20}$$

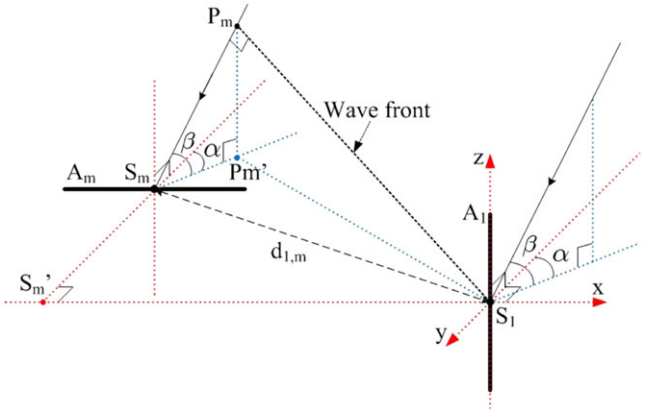

FIGURE 9 3-D multipolarized uniform circular array massive multiple-input multiple-output system transmission scenario

where $\angle S_m^{'} S_m S_1 = \arctan(\frac{S_m^{'} S_1}{S_m S_m^{'}})$ and $S_m^{'} S_1$, $S_m S_m^{'}$ are the functions of antenna spacing d and the number of antennas. Then for different antennas, we have

$$\begin{aligned} S_2^{'} S_1 &= r\sin\theta_2, S_2 S_2^{'} = r - r\cos\theta_2 \\ &\cdots \\ S_m^{'} S_1 &= r\sin\theta_m, S_m S_m^{'} = r - r\cos\theta_m \\ &\cdots \end{aligned} \tag{21}$$

Regarding vertically polarized antenna A_1 as a reference antenna, for horizontally polarized antenna A_m, one path of multipath channels of multipolarized UCA massive MIMO systems can be expressed as

$$h_1^{\mathrm{UCA,XPD}} = \sqrt{P_{\mathrm{V}}(1-a) + P_{\mathrm{H}} a} e^{j\phi} \tag{22}$$

$$\begin{aligned} h_m^{\mathrm{UCA,XPD}} &= \sqrt{P_{\mathrm{H}}(1-a) + P_{\mathrm{V}} a} \\ &\quad \times e^{j(\phi + 2\pi d_{1,m}\cos(\pi - \alpha - \arctan(\frac{r\sin\theta_m}{r - r\cos\theta_m}))\cos(\beta)/\lambda)}. \end{aligned} \tag{23}$$

Then the channel vectors of user p with single vertically polarized antenna and user q with single horizontally polarized antenna for multipolarized UCA massive MIMO systems can be written as (18) and (19). Also we can get the channel orthogonality and channel capacity of multipolarized UCA massive MIMO systems as multipolarized ULA massive MIMO systems.

$$\mathbf{h}_p^{\mathrm{URA,XPD}} = \begin{bmatrix} h_{11,p}^{\mathrm{URA,XPD}} \\ h_{12,p}^{\mathrm{URA,XPD}} \\ \cdots \\ h_{21,p}^{\mathrm{URA,XPD}} \\ \cdots \\ h_{mn,p}^{\mathrm{URA,XPD}} \\ \cdots \end{bmatrix} = \begin{bmatrix} \sqrt{P_{\mathrm{V}}(1-a)} e^{j\phi_p} \\ \sqrt{P_{\mathrm{V}} a} e^{j(\phi_p + 2\pi d\cos(\pi/2 - \alpha_p)\cos(\beta_p))/\lambda)} \\ \cdots \\ \sqrt{P_{\mathrm{V}} a} e^{j(\phi_p - 2\pi d\cos(\pi/2 - \beta_p))/\lambda)} \\ \cdots \\ \sqrt{P_{\mathrm{V}} a} e^{j(\phi_p + 2\pi((n-1)d\cos(\pi/2 - \alpha_p)\cos(\beta_p) - (m-1)d\cos(\pi/2 - \beta_p)))/\lambda)} \\ \cdots \end{bmatrix}, \tag{24}$$

$$\mathbf{h}_q^{\mathrm{URA,XPD}} = \begin{bmatrix} h_{11,q}^{\mathrm{URA,XPD}} \\ h_{12,q}^{\mathrm{URA,XPD}} \\ \cdots \\ h_{21,q}^{\mathrm{URA,XPD}} \\ \cdots \\ h_{mn,q}^{\mathrm{URA,XPD}} \\ \cdots \end{bmatrix} = \begin{bmatrix} \sqrt{P_{\mathrm{H}} a} e^{j\phi_q} \\ \sqrt{P_{\mathrm{H}}(1-a)} e^{j(\phi_q + 2\pi d\cos(\pi/2 - \alpha_q)\cos(\beta_q))/\lambda)} \\ \cdots \\ \sqrt{P_{\mathrm{H}}(1-a)} e^{j(\phi_q - 2\pi d\cos(\pi/2 - \beta_q))/\lambda)} \\ \cdots \\ \sqrt{P_{\mathrm{H}}(1-a)} e^{j(\phi_q + 2\pi((n-1)d\cos(\pi/2 - \alpha_q)\cos(\beta_q) - (m-1)d\cos(\pi/2 - \beta_q)))/\lambda)} \\ \cdots \end{bmatrix}. \tag{25}$$

4 | 3-D CHANNEL MODELING OF MULTIPOLARIZED URA MASSIVE MIMO SYSTEMS

For massive MIMO systems, the URA antenna structure is also widely used. Our proposed scheme for multipolarized URA massive MIMO systems is shown in Figure 10. Both the horizontally and vertically adjacent antenna spacing is d, [7] and any 2 adjacent antennas must have different polarizations. The channel model analysis of multipolarized URA massive MIMO systems is a little more complex than the ULA and the UCA. Also, we first analyze the relationship between 2 antennas A_{11} and A_{mn} as shown in Figure 11. Figure 11 is the 2 antennas in the far field of the signals, and the transmission distance difference between the 2 antennas is

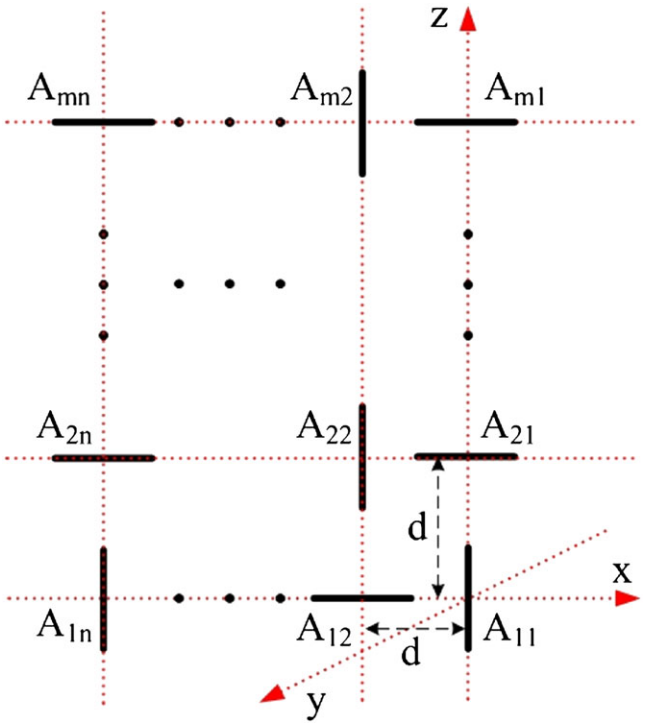

FIGURE 10 Multipolarized uniform rectangular array massive multiple-input multiple-output system antenna structure

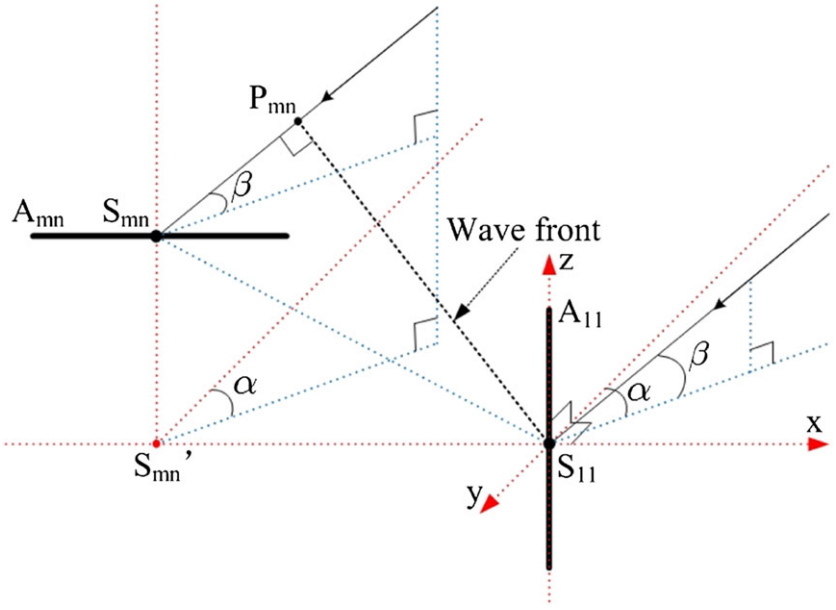

FIGURE 11 3-D multipolarized uniform rectangular array massive multiple-input multiple-output system transmission scenario

$$\begin{aligned} S_{mn}P_{mn} &= S'_{mn}S_{11}\cos(\pi/2-\alpha)\cos(\beta) \\ &\quad -S_{mn}S'_{mn}\cos(\pi/2-\beta). \end{aligned} \tag{26}$$

Since all the antennas are uniformly spaced in both horizontal and vertical directions, $S_{mn}S'_{mn}$ and $S'_{mn}S_{11}$ are the multiples of the adjacent antenna spacing d. Regarding antenna A_{11} as a reference antenna, one path of multipath channels of multipolarized URA massive MIMO systems can be expressed as

$$h_{11}^{\mathrm{URA,XPD}} = \sqrt{P_{\mathrm{V}}(1-a)+P_{\mathrm{H}}a}e^{j\phi} \tag{27}$$

$$h_{mn}^{\mathrm{URA,XPD}} = \sqrt{P_{\mathrm{H}}(1-a)+P_{\mathrm{V}}a} \times e^{j(\phi+2\pi((n-1)d\cos(\pi/2-\alpha)\cos(\beta)-(m-1)d\cos(\pi/2-\beta)))/\lambda}. \quad (28)$$

The channel vectors of user p with single vertically polarized antenna and user q with single horizontally polarized antenna for multipolarized URA massive MIMO systems can be written as (24) and (25). Then we can get the channel orthogonality and channel capacity of multipolarized URA massive MIMO systems as multipolarized ULA massive MIMO systems.

5 | SIMULATION RESULT COMPARISONS AND ANALYSIS

For the parameters AAS, antenna spacing, XPD, SNR, and k-factor, the multipolarized UCA and URA massive MIMO systems have the same performance as multipolarized ULA massive MIMO systems, which are not shown again. Like the multipolarized ULA massive MIMO systems, the multipolarized UCA and URA massive MIMO systems also have better performance than the unipolarized counterparts as shown in Figure 12A. The antenna spacing is set to be $\lambda/2$,

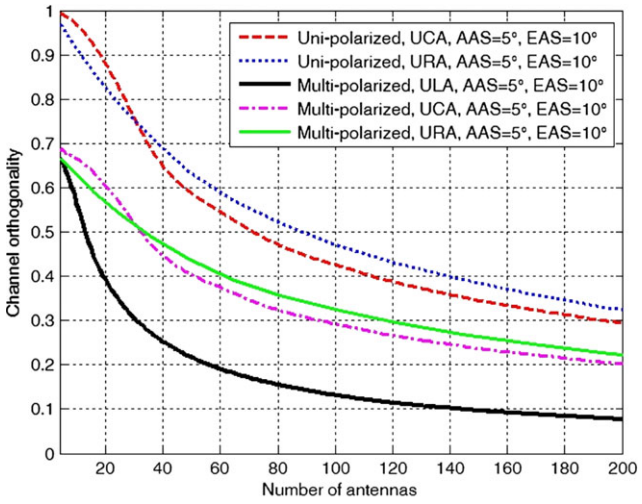

(A)

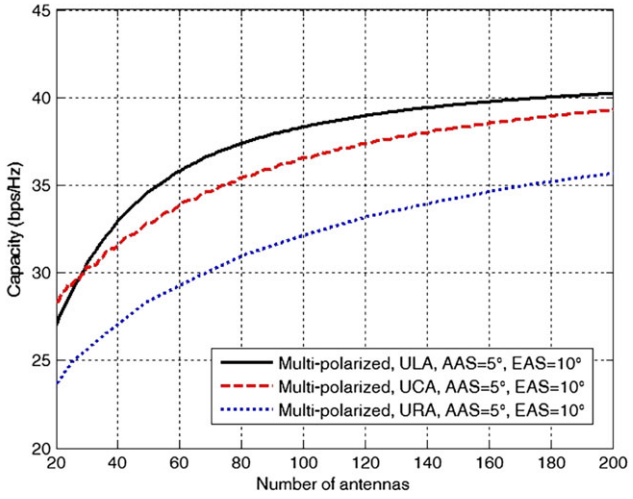

(B)

FIGURE 12 A, Channel orthogonality comparison of multipolarized ULA, UCA, and URA massive multiple-input multiple-output systems versus number of antennas. B, Channel capacity comparison of multipolarized ULA, UCA, and URA massive multiple-input multiple-output systems versus number of antennas. AAS, azimuth angle spread; EAS, elevation angle spread; UCA, uniform circular array; ULA, uniform linear array; URA, uniform rectangular array

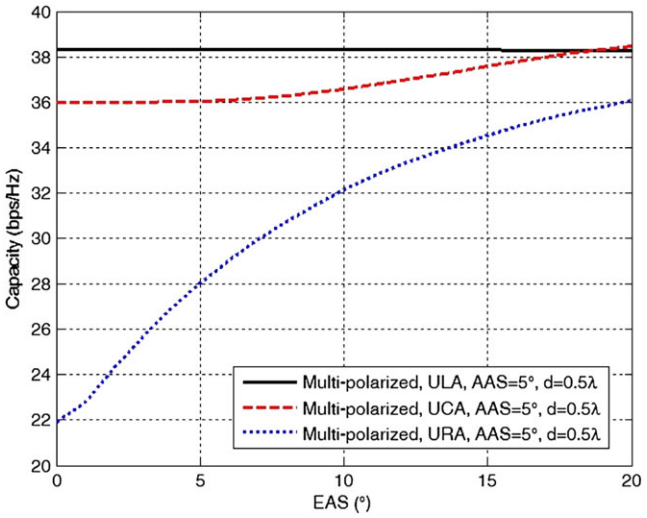

FIGURE 13 Channel capacity comparison of multipolarized ULA, UCA, and URA massive multiple-input multiple-output systems versus EAS. AAS, azimuth angle spread; EAS, elevation angle spread; UCA, uniform circular array; ULA, uniform linear array; URA, uniform rectangular array

and XPD is equal to 8 dB. For multipolarized URA massive MIMO systems, we use the square antenna structure by setting $m = n$. From Figure 12A, we can see that multipolarized antennas can be also used in UCA and URA massive MIMO systems to decline the channel orthogonality. The multipolarized ULA massive MIMO systems have the lowest channel orthogonality while the multipolarized URA massive MIMO systems have the highest channel orthogonality. This is because the multipolarized ULA massive MIMO systems have a long line antenna structure with more space resulting in low channel orthogonality and multipolarized URA massive MIMO systems are more compact with small space resulting in high channel orthogonality. Figure 12B compares the channel capacity of multipolarized ULA, UCA, and URA massive MIMO systems versus number of antennas. Signal-to-noise ratio is set to be 20 dB, *k*-factor equals to 0 dB to avoid any part becomes dominated, and the power is equally allocated. All the channel capacities increase as the number of antennas increases. The multipolarized ULA massive MIMO systems have the highest channel capacity because of the lowest channel orthogonality, while the multipolarized URA massive MIMO systems have the lowest channel capacity because of the highest channel orthogonality. Figure 13 shows that multipolarized ULA massive MIMO systems are not sensitive to the EAS while the channel capacity of multipolarized UCA and URA massive MIMO systems is increased as EAS increases. This is because the multipolarized ULA massive MIMO systems are 1-dimensional antenna structure placed in just one line and the multipolarized UCA and URA massive MIMO systems are 2-dimensional antenna structure placed in the horizontal or vertical plane; therefore, the large EAS can bring them more scattering to enhance the performance especially for the multipolarized URA massive MIMO systems.

6 | CONCLUSION

In this paper, we implemented the multipolarized antennas in massive MIMO systems to improve the systems performance and establish 3-D geometrical channel models for the proposed multipolarized massive MIMO systems. Using multipolarized antennas in massive MIMO systems can help to decline the channel orthogonality between users and reduce the demand for large antenna spacing to realize the space efficiency. The multipolarized massive MIMO systems have better performance than the unipolarized massive MIMO systems in many situations. Also, the multipolarized antennas implemented in massive MIMO systems cause the power loss and imbalance between antennas. Therefore, the multipolarized massive MIMO systems do not outperform unipolarized massive MIMO systems when SNR is low. Finally, if the space efficiency and the miniaturization of equipments are of primary concern, the multipolarized antennas would be the best choice for massive MIMO systems.

ACKNOWLEDGEMENTS

This work was supported in part by the National Natural Science Foundation of China under grant 61372077, in part by the Shenzhen Science and Technology Programs under grants ZDSYS 201507031550105, JCYJ 20170302150411789, JCYJ 20170302142515949, and GCZX 2017040715180580, and in part by the Guangdong Provincial Science and Technology Program under grant 2016B090918080, and in part by China Postdoctoral Science Foundation under grant 2016M602519, as well as Guangzhou Science and Technology Program under grant 201707010490.

ORCID

Yejun He http://orcid.org/0000-0002-8564-5355

REFERENCES

1. Marzetta TL. Noncooperative cellular wireless with unlimited numbers of base station antennas. *IEEE Trans Wirel Commun*. 2010;9(11):3590-3600.
2. Marzetta TL. Massive MIMO: an introduction. *Bell Labs Tech J*. 2015;20:11-22.
3. Gao X, Edfors O, Rusek F, Tufvesson F. Linear pre-coding performance in measured very-large MIMO channels. In: Proc. 2011 IEEE Vehicular Technology Conference (VTC Fall); September 2011; San Francisco, CA, USA:1-5.
4. Zheng K, Ou S, Yin X. Massive MIMO channel models: a survey. *Int J Antennas Propag*. 2014;11:1-10.
5. Wu X, Beaulieu NC, Liu D. On favorable propagation in massive MIMO systems and different antenna configurations. *IEEE Access*. 2017;5:5578-5593.
6. Varzakas P. Average channel capacity for Rayleigh fading spread spectrum MIMO systems. *Int J Commun Syst*. 2006;19(10):1081-1087.
7. Gauger M, Hoydis J, Hoek C, Schlesinger H, Pascht A, ten Brink S. Channel measurements with different antenna array geometries for massive MIMO systems. In: Proc. 2015 10th International ITG Conference on Systems, Communications and Coding (SCC); February 2015; Hamburg, Germany:1-6.
8. Park J, Clerckx B. Multi-user linear precoding for multi-polarized massive MIMO system under imperfect CSIT. *IEEE Trans Wirel Commun*. 2015;14(5):2532-2547.
9. Erceg V, Baum D, Pitchaiah S, Paulraj AJ. Capacity obtained from multiple-input multiple-output channel measurements in fixed wireless environments at 2.5 GHz. In: Proc. 2002 IEEE International Conference on Communications(ICC); May 2002; New York, USA:396-400.
10. Gao X, Edfors O, Rusek F, Tufvesson F. Massive MIMO performance evaluation based on measured propagation data. *IEEE Trans Wirel Commun*. 2015;14(7):3899-3911.
11. Flordelis J, Gao X, Dahman G, Rusek F, Edfors O, Tufvesson F. Spatial separation of closely-spaced users in measured massive multi-user MIMO channels. In: Proc. 2015 IEEE International Conference on Communications (ICC); June 2015; London, UK:1441-1446.
12. Hoydis J, Hoek C, Wild T, ten Brink S. Channel measurements for large antenna arrays. In: Proc. 2012 International Symposium on Wireless Communication Systems (ISWCS); August 2012; Paris, France:811-815.
13. Payami S, Tufvesson F. Channel measurements and analysis for very large array systems at 2.6 GHz. In: Proc. 2012 6th European Conference on Antennas and Propagation (EUCAP); March 2012; Prague, Czech Republic:433-437.
14. Li J, Zhao Y, Tan Z. Indoor channel measurements and analysis of a large-scale antenna system at 5.6 GHz. In: Proc. 2014 IEEE/CIC International Conference on Communications in China (ICCC); October 2014; Shanghai, China:281-285.
15. Wu S, Wang C, Aggoune el-HM, Alwakeel MM, He Y. A non-stationary 3-D wideband twin-cluster model for 5G massive MIMO channels. *IEEE J Sel Areas Commun*. 2014;32(6):1207-1218.
16. Xie Y, Li B, Zuo X, Yang M, Yan Z. A 3D geometry-based stochastic model for 5G massive MIMO channels. In: Proc. 2015 11th International Conference on Heterogeneous Networking for Quality, Reliability, Security and Robustness (QSHINE); August 2015; Taipei, Taiwan:216-222.
17. Li X, Zhou S, Bjornson E, Wang J. Capacity analysis for spatially non-wide sense stationary uplink massive MIMO systems. *IEEE Trans Wirel Commun*. 2015;14(12):7044-7056.
18. Nguyen SLH, Haneda K, Jarvelainen J, Karttunen A. On the mutual orthogonality of millimeter-wave massive MIMO channels. In: Proc. 2015 IEEE 81st Vehicular Technology Conference (VTC Spring); May 2015; Glasgow, UK:1-5.
19. Li J, Zhao Y. Channel characterization and modeling for large-scale antenna systems. In: Proc. 2014 14th International Symposium on Communications and Information Technologies (ISCIT); September 2014; Incheon, South Korea:559-563.

20. Xu W, Wu X, Dong X, Zhang H, You X. Dual-polarized massive MIMO systems under multi-cell pilot contamination. *IEEE Access*. 2016;4:5998-6013.
21. Xiao H, Chen Y, Li Y, Lu Z. CSI feedback for massive MIMO system with dual-polarized antennas. In: Proc. 2015 IEEE 26th Annual International Symposium on Personal, Indoor, and Mobile Radio Communications (PIMRC); September 2015; Hong Kong, China:2324-2328.
22. Coldrey M. Modeling and capacity of polarized MIMO channels. In: Proc. 2008 IEEE Vehicular Technology Conference(VTC); May 2008; Singapore:440-444.
23. Quoc NH, Larsson EG, Marzetta TL. Aspects of favorable propagation in massive MIMO. In: Proc. 2014 Proceedings of the 22nd European Signal Processing Conference (EUSIPCO); September 2014; Lisbon, Portugal:76-80.
24. He Y, Cheng X, Stüber GL. On polarization channel modeling. *IEEE Wirel Commun*. 2016;23(1):80-86.
25. Cheng X, He Y. Geometrical model for massive MIMO systems. In: Proc. 2017 IEEE 85th Vehicular Technology Conference (VTC2017 Spring); September 2017; Sydney, NSW, Australia:1-6.
26. Kwon S, Stüber GL. Geometrical theory of channel depolarization. *IEEE Trans Veh Technol*. 2011;60(8):3542-3556.
27. Jiang L, Thiele L, Jungnickel V. On the modelling of polarized MIMO channel. In: Proc. IEEE European Wireless Conference; April 2007; Prague, Czech Republic:1-6.
28. Ma Y, Zheng Z, Zhou Yl. Characteristics of MIMO channel in consideration of polarization. In: Proc. Wireless Communications, Networking and Mobile Computing; 2009; Beijing, China:1-3.
29. Liu L, Matolak DW, Tao C, Li Y, Ai B, Houjin C. Channel capacity investigation of a linear massive MIMO system using spherical wave model in LOS scenarios. *Sci China Inf Sci*. 2016;59(2):1-15.
30. Gao X, Tufvesson F, Edfors O, Rusek F. Measured propagation characteristics for very-large MIMO at 2.6 GHz. In: Proc. 2012 Conference Record of the Forty Sixth Asilomar Conference on Signals, Systems and Computers (ASILOMAR); November 2012; Pacific Grove, CA, USA:295-299.
31. Cho YS, Kim J, Yang WY, Kang CG. *MIMO-OFDM Wireless Communication Technology with MATLAB*. Beijing: Publishing House of Electronics Industry; 2013.
32. Soma P, Baum DS, Erceg V, Krishnamoorthy R, Paulraj AJ. Analysis and modeling of multiple-input multiple-output (MIMO) radio channel based on outdoor measurements conducted at 2.5 GHz for fixed BWA applications. In: Proc. 2002 IEEE International Conference on Communications(ICC); May 2002; New York, USA:272-276.
33. Dao M, Nguyen V, Im Y, Park S, Giwan Y. 3D polarized channel modeling and performance comparison of MIMO antenna configurations with different polarizations. *IEEE Trans Antennas Propag*. 2011;59(7):2672-2682.

How to cite this article: Cheng X, He Y, Zhang L, Qiao J. Channel modeling and analysis for multipolarized massive MIMO systems. *Int J Commun Syst*. 2018;31:e3703. https://doi.org/10.1002/dac.3703